Fabrication of ZnO-Carbon Dots Composite *via* Microcrystalline Cellulose for Enhanced Photocatalytic Hydrogen Production under Simulated Sunlight Irradiation

Xiangyu Li,[a,#] Wanquan Hu,[a,#] Shuo Qiao,[a,#] Yuexin Chang,[a] Longxiao Gu,[a] Yang Wang,[b,]* Hui-Liang Sun,[a,]* and Yuan-Ru Guo [a,]*

** Corresponding authors: guoyrnefu@163.com; 18745015921@126.com; 414778430@qq.com*

DOI: 10.15376/biores.19.3.5511-5522

GRAPHICAL ABSTRACT

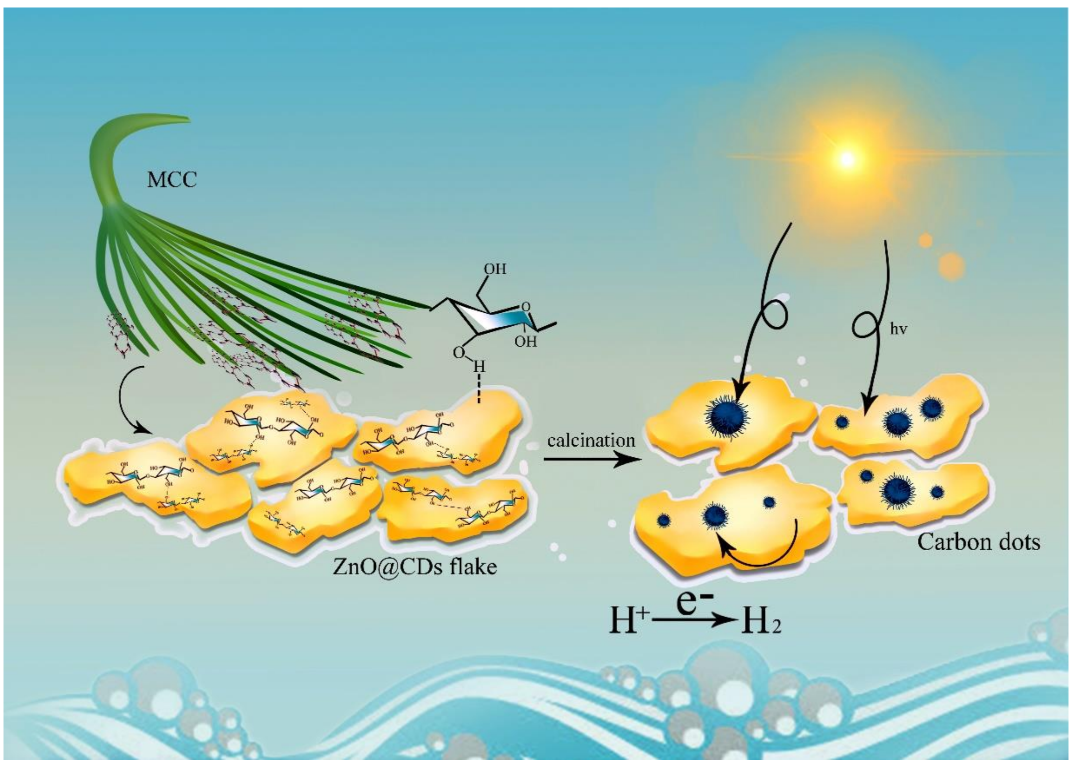

Fabrication of ZnO-Carbon Dots Composite *via* Microcrystalline Cellulose for Enhanced Photocatalytic Hydrogen Production under Simulated Sunlight Irradiation

Xiangyu Li,[a,#] Wanquan Hu,[a,#] Shuo Qiao,[a,#] Yuexin Chang,[a] Longxiao Gu,[a] Yang Wang,[b,]* Hui-Liang Sun,[a,]* and Yuan-Ru Guo [a,]*

The composite ZnO@CDs was prepared *via* the hydrothermal method. Microcrystalline cellulose (MCC) was used as the source of carbon dots (CDs). X-ray diffraction, Fourier transform infrared spectrometry, scanning electron microscopy, and transmission electron microscopy analyses were used to characterize the structure and morphology of ZnO@CDs. The prepared ZnO showed a flake morphology with the exposed plane of (001). The X-ray photoelectron spectroscopy and photoluminescence spectroscopy (PL) characterization showed that CDs can be produced by decomposition of MCC and then attached on the surface of ZnO. The photocatalytic properties of ZnO@CDs were investigated under simulated sunlight irradiation. The hydrogen production reached 1240 $\mu mol \cdot g^{-1}$ in 30 min, which was much higher than the bare ZnO. The mechanism for the enhanced catalytic property of ZnO@CDs was studied. A high hydrogen production rate (2480 $\mu mol \cdot g^{-1} \cdot h^{-1}$) in the short term would enable ZnO@CDs to work as an emergency power supply by hydrogen production and use for restoring electricity and wireless communication in complicated situations.

DOI: 10.15376/biores.19.3.5511-5522

Keywords: ZnO; CDs; Microcrystalline cellulose; Photocatalysis; Hydrogen production

Contact information: a: Key Laboratory of Bio-based Material Science & Technology (Ministry of Education), College of Material Science and Engineering, Northeast Forestry University, Harbin 150040, China; b: Harbin Centre for Disease Control and Prevention (Harbin Centre for Health Examination), Harbin 150030, China; [#]These three authors contributed to the work equally;
**Corresponding authors: 18745015921@126.com; 414778430@qq.com; guoyrnefu@163.com*

INTRODUCTION

In the face of the increasingly dire energy crisis and environmental problems, reducing carbon emissions by converting solar energy into usable clean hydrogen energy has become a key topic of concern (Raza and Ahmad 2022; Raza *et al*. 2023). Due to their appropriate band gap and redox properties, certain semiconductors have shown great potential as photocatalysts for water splitting. ZnO, which has high electron mobility, strong oxidation, as well as nontoxicity, has been widely studied as a photocatalyst. It is reported that ZnO has a unique surface effect, and it achieves higher quantum efficiency than the traditional TiO_2 (Guo *et al*. 2013). However, ZnO has a band gap of 3.37, which makes it difficult to harvest visible light efficiently (Wang 2004; Barman *et al*. 2017). Additionally, the electron-hole pairs recombine easily during the optical radiation process, which greatly restricts the application of ZnO for H_2 evolution (Raza *et al*. 2014; Trang *et al*. 2020).

Many strategies have been adopted to improve the photocatalytic property of ZnO, such as an increase of the separation efficiency of charge carriers or widening light absorption range (Luo *et al*. 2019; Raza *et al*. 2023). The construction of S-scheme heterojunctions is believed to be an effective method. ZnO composites with S-scheme heterojunction, such as ZnO/ZnS, ZnO/CdS, and so forth, were studied. Results have shown that the S-scheme heterojunction can inhibit the combination of electron-hole pairs in composite and improve its properties. Though this method can improve the water-splitting efficiency of ZnO, the complicated preparation method restricts its further application.

Surface modification is another strategy for the improvement of the photocatalytic property of ZnO. Introducing materials with good conductivity on the surface of ZnO is an effective way to improve its photocatalytic property. Noble metals, such as Ag (Raza *et al*. 2023) or Ru (Chen *et al*. 2005; Vaiano and Iervolino 2019), can transfer the photogenerated electrons away and then improve the H_2 production rate by increasing the separation rate of electron-hole pairs. However, the high price of these noble metals is a barrier to their application. A cost-effective surface modification material with good conductivity for photocatalyst is still in demand.

As a regenerative biomass resource, cellulose has the advantages of abundance, degradability, and low cost (Zhang *et al*. 2021). Because cellulose molecules were formed by chemically linked D-glucopyranose units, there are plenty of hydroxyl groups in its structure (Chauhan *et al*. 2015; Liu *et al*. 2016; Zhao *et al*. 2017; Wang *et al*. 2021). This character enables cellulose to build hydrogen bonds with ZnO easily and then influence its morphology and microstructure. Thus, some research has been carried out to prepare cellulose-based ZnO composite, and properties of antibacterial activity, adsorption, and UV shielding have been studied. However, most of the studies on ZnO/cellulose have focused on the dispersion of ZnO by cellulose. As a bioresource, cellulose can decompose into carbon dots (CDs) during hydrothermal synthesis at high temperature (Li *et al*. 2023; Balanta *et al*. 2023). There has been a lack of work in which prepared ZnO has been coated with cellulose-derived CDs. Thus, the prepared ZnO@CDs photocatalyst for H_2 production would provide a new strategy for sustainable development.

As a typical zero-dimensional nanomaterial, CDs have attracted a lot of researchers' interests due to their superior physicochemical properties, easy preparation, and environmental friendliness (Tang *et al*. 2024). Recently, CDs prepared from biomass materials have been widely studied, such as from sucrose (Pan *et al*. 2018) or cellulose (Han *et al*. 2018). When combined with metal oxides, abundant O active sites in CDs can provide an "empty house" for the electrons jumping out of the photoexcitation and then improve the separate rate of electrons and hole pairs. Thus, favorable results would be achieved. Due to this character, CDs have been applied to combine with semiconductors such as Fe_2O_3 (Ying *et al*. 2023), TiO_2 (Zhao *et al*. 2021), and ZnO (Pan *et al*. 2018). Samples of CDs/ZnO and TiO_2/CDs prepared by coconut and glucosamine hydrochloride showed enhanced photocatalytic properties for degradation of antibiotics and reactive red azo dyes (Zhao *et al*. 2021; Nugroho *et al.* 2024). Thus, CDs are expected to replace the traditional semiconductor quantum dots in photocatalyst compounding (Guo *et al*. 2013).

Due to the relatively small size and abundance of hydroxyl groups of the microcrystalline cellulose (MCC), it was applied to fabricate the ZnO/CDs/MCC composite *via* a hydrothermal method. As a result of the calcination, MCC was no longer present, and ZnO/CDs were obtained. The morphology, structure, and the H_2 evolution performance of ZnO/CDs were studied. The results show that ZnO@CDs photocatalysts exhibited excellent catalytic efficiency for hydrogen production under both visible light and simulated sunlight irradiation.

EXPERIMENTAL

Reagents and Chemicals

Microcrystalline cellulose (20 to 100 μm) was provided by Tianjin Guangfu Fine Chemical Research Institute. Zinc acetate dihydrate, sodium hydroxide, and methanol were purchased from Tianda Chemical Reagent Factory in Dongli District.

Synthesis of ZnO@CDs

A total of 1.0 g of MCC and 1.6 g of zinc acetate dihydrate were put into 25 mL deionized water and stirred for 30 min. Next, 5 mol/L NaOH solution was added into the mixture to make the pH of the solution 11. After 30 min stirring, the mixture was transferred into a steel reactor with PTFE substrate and heated at 160 ℃ for 10 h. After cooling to room temperature, the ZnO@CDs/MCC was obtained by centrifugal washing (8000rmp and 5 min for 3 times), which was followed by drying at 50 ℃ in a vacuum drying oven. Finally, ZnO@CDs was obtained after calcined at 550 ℃ for 2 h in a muffle furnace with the hearting rate of 5^o min^{-1} in air condition.

To investigate the effect of hydrothermal temperature on the photocatalytic property of ZnO@CDs, hydrothermal temperatures of 100, 140, 160, and 180 ℃ were taken into consideration. The products were named ZnO@CDs-100, ZnO@CDs-140, ZnO@CDs-160, and ZnO@CDs-180 according to their preparation temperature.

Characterization

Multiple techniques are used to characterize the structure and performance of photocatalysts. The crystal structures of the samples were analyzed by X-ray diffraction (XRD; D/max-RC, Rigaku, Japan) with Cu Kα (λ = 1.5418 Å) within a 2θ range of 10° to 80°. Elemental analysis and bonding information on the sample were tested using X-ray photoelectron spectroscopy (XPS; K-Alpha, Thermo Fisher, Waltham, MA, USA). High-resolution transmission electron microscopy (HRTEM; JEM-2100, JEOL, Tokyo, Japan) and scanning electron microscopy (SEM; JSM-7500F, JEOL, Japan) were used to study the microstructure and morphology of the samples, respectively. The Fourier transform infrared spectroscopy (FTIR; Frontier, PerkinElmer, Shelton, CT, USA) was recorded within the range of 600 to 3900 cm^{-1} and was used to analyze functional groups of samples. The Electrochemical Impedance Spectroscopy (EIS) was tested by an electrochemical workstation (CHI760E, CH Instruments Inc., Bee Cave, TX, USA).

Photocatalytic H_2 Generation *via* Water Splitting

A total of 20 mg ZnO@CDs was mixed with a 100 mL methanol-water mixture (1:1, volume) in a 250 mL reactor, and then the system was pumped close to a vacuum condition. Xenon lamp light (300W) with a filter (AM1.5) was used as the light source. An online detection system of absolar-6A (Perfect Lingt, China) equipped with Agilent 8860 Gas chromatography (GC) was used to extract the gas in the reaction system every 30 min and test the hydrogen production volume automatically. The modality of the test was continuous.

RESULTS AND DISCUSSION

Structural Characterization

The structure of ZnO@CDs was studied by XRD, and results are shown in Fig. 1a. It can be seen that diffraction peaks were located at 2θ of 31.7°, 34.5°, 36.2°, 47.5°, 56.6°, and 62.8°, corresponding to the crystal planes of (100), (002), (101), (102), (110), and (103) of hexagonal wurtzite ZnO (PDF#99-0111). The strong and sharp diffraction peaks indicate that the ZnO@CDs photocatalyst had a high degree of crystallinity. Because the XRD patterns of ZnO@CDs-100~ZnO@CDs-180 were very close to each other, it is deduced that different hydrothermal temperatures did not influence the structure of ZnO. However, the phase of CDs was not found in all XRD patterns. This may be caused by the low contents of CDs in the composite, though it may be influenced by temperature.

The FTIR spectra of ZnO, ZnO@CDs/MCC, and ZnO@CDs are shown in Fig. 1b. In the case of the bare ZnO, there were almost no characteristic absorbance peaks in its spectra. However, the ZnO@CDs/MCC showed more complicated absorbance peaks: the wide band peak centered at 3335 cm^{-1} is -OH stretching vibrational absorption; and the peak at 1031 cm^{-1} is the C-O-C characteristic absorbance peak, which is a typical oxygen-containing functional group of cellulose. Meanwhile, the absorbance peak at 2889 cm^{-1} is attributed to the C-H stretching vibrational absorbance peaks. Moreover, the peak at 1647 cm^{-1} is the absorbance peak of water. To the IR spectrum of ZnO@CDs, absorbance peak of water disappeared after calcination. There is a broad absorbance band centered at 3335 cm^{-1}, which corresponds to -OH vibration. This result indicated that there are plenty of -OH groups in ZnO@CDs compared to bare ZnO, which originated from the CDs in the composite. Meanwhile, the characteristic peak at 2321 cm^{-1} is a signal of CO_2, which was adsorbed on the sample (Wang *et al*. 2019). The adsorption peaks located at 1517 cm^{-1} and 1371 cm^{-1} are C=C-C=O and O–H bending vibrations (Jamal *et al*. 2020).

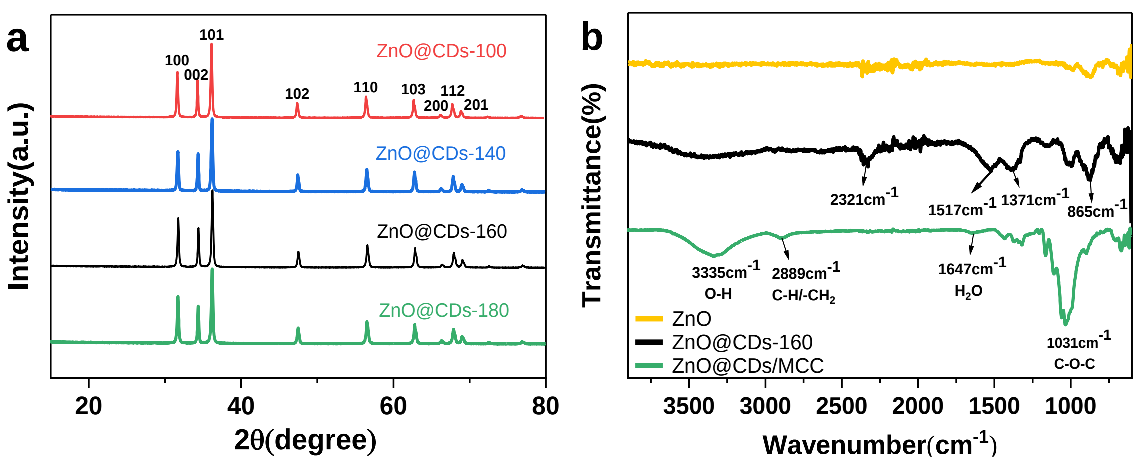

Fig. 1. (a) XRD patterns of ZnO@CDs; (b) FTIR images of ZnO@CDs/MCC, ZnO@CDs-160, and ZnO

The morphology of ZnO@CDs was studied by SEM. It can be seen from Fig. 2a through 2d that all ZnO@CDs showed flake morphology. The width of these flakes was about 300 nm, and the thickness was within 100 nm. It is worth mentioning that a higher hydrothermal temperature resulted in thinner ZnO@CDs. This may be caused by the interaction between the MCC and ZnO during the hydrothermal process. High temperature makes MCC and ZnO nanocrystals easy to build interface interaction and block the growth of ZnO. To further explore this finding, the TEM of ZnO@CDs-160 was tested, and the pictures are listed in Fig. 2e through 2g. From the pictures, it can be seen that ZnO@CDs were in the form of thin flakes, which is consistent with the SEM result. The high-resolution picture of ZnO@CDs gives the clear lattice fringe, and the interplanar spacing was measured to be 0.261 nm according to Fig. 2g. Because the 0.261 nm is the spacing of (002) plane, it is apparent that the (001) plane of ZnO was exposed after calcination. Because the (001) plane of ZnO has higher energy than the other planes, it was deduced that as-prepared ZnO@CDs would have good photocatalytic properties.

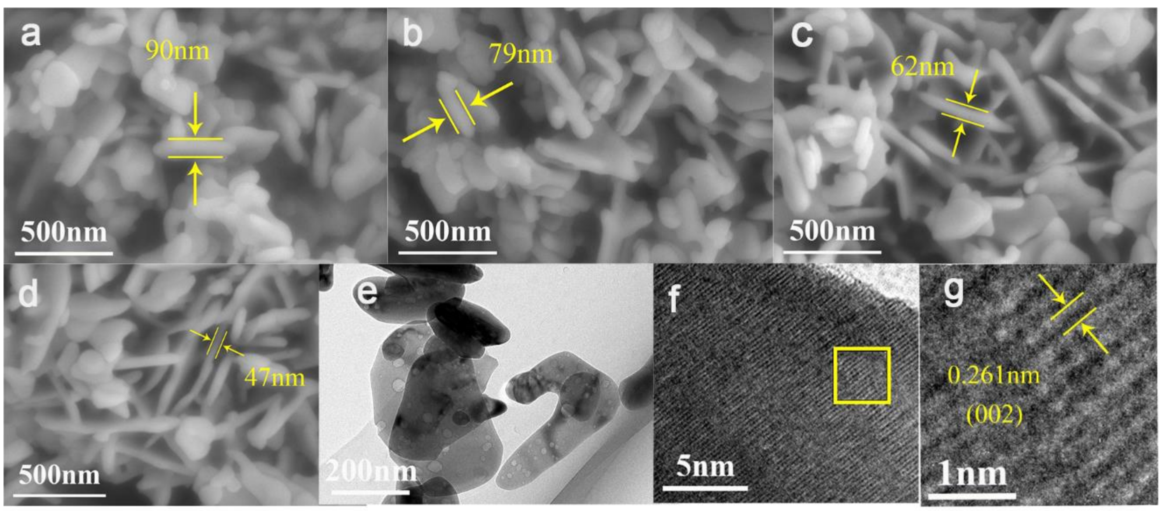

Fig. 2. SEM images of (a) ZnO@CDs-100, (b) ZnO@CDs-140, (c) ZnO@CDs-160, (d) ZnO@CDs-180; and HRTEM images of (e through g) ZnO@CDs-160

The XPS method was used to analyze the elemental chemical environment of ZnO@CDs. Figure 3a shows the XPS survey spectrum and only peaks of Zn, O, and C are found. This result indicated that the composite was composed of these three elements. The XPS spectrum of Zn 2p (Fig. 3b) shows a doublet at 1021.5 and 1044.7 eV. It can be attributed to the 2p3/2 and 2p1/2 of divalent Zn (Wu *et al*. 2013). Figure 3c shows the high-resolution XPS spectrum of O1s, and two peaks could be fitted. The peak at 530.2 eV was attributed to the lattice oxygen of ZnO crystal (Trang *et al*. 2020); and the peak at 532.2 eV can be assigned to the binding energy of C-O and C=O originated from CDs. This gave evidence that CDs were present in the composite. The XPS spectrum of C1s also gave the same evidence, as shown in Fig. 3d. There were two peaks that can be observed at 284.2 and 288.1 eV after fitting, which are binding energies of C-C/C=C and C-O/C=O originating from CDs. This result indicates that CDs were attached on the surface of ZnO photocatalysts successfully.

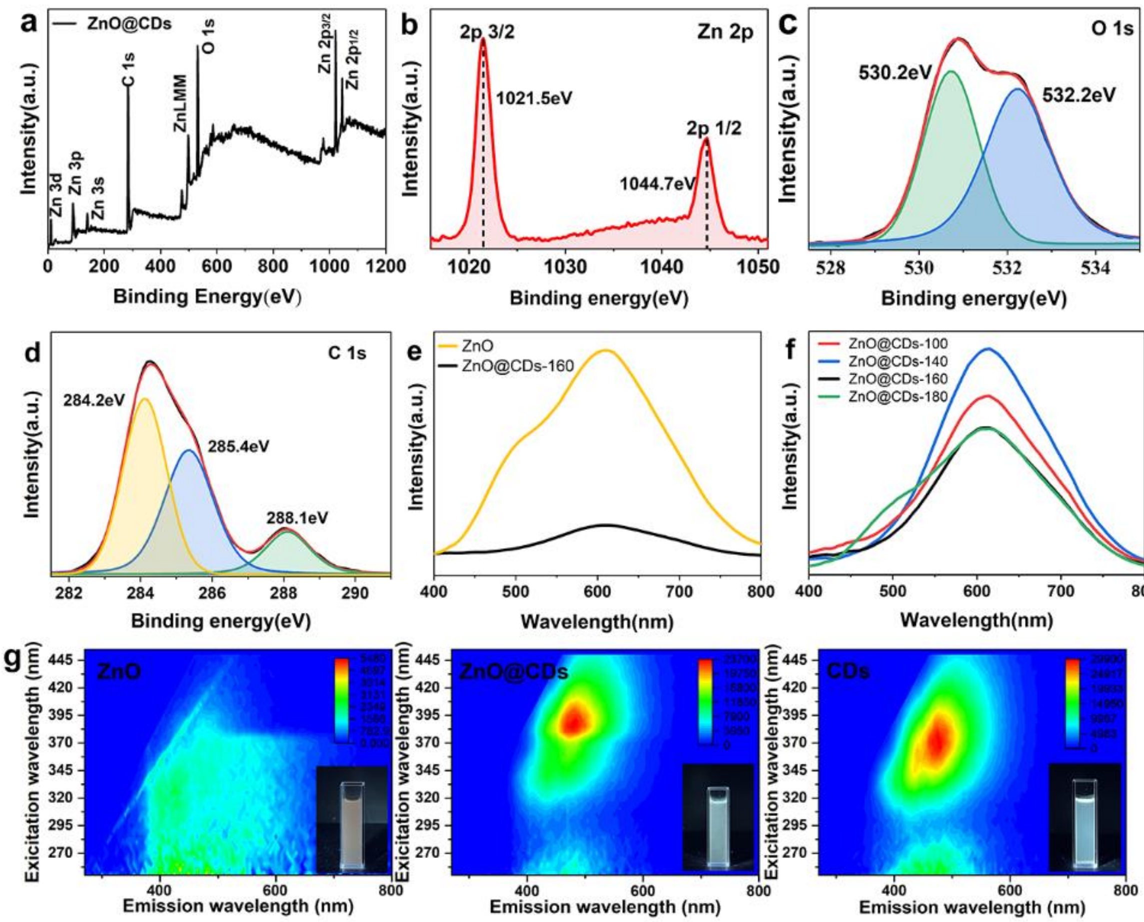

Fig. 3. XPS spectra of ZnO@CDs: (a) survey, (b) Zn 2p, (c) O 1s, and (d) C 1s; PL spectra (e) ZnO and ZnO@CDs, (f) ZnO@CDs prepared at different temperature, (g) PL emission spectra at different excitation wavelength for ZnO suspension, ZnO@CDs suspension and CDs solution, the insert pictures are fluorescence pictures taken under 365 nm irradiation.

To study the migration dynamics of photoluminescent carriers, PL photoluminescence spectra of ZnO@CDs were tested under 350 nm excitation wavelength, and the results are shown in Figs. 3e and 3f. According to previous studies, ZnO usually has two emission peaks: UV emission and visible PL emission. Because the visible light and simulated sunlight were considered as light sources in this experiment, the visible PL emission from 400 to 800 nm was of concern in this work. There was a wide band visible PL emission in Fig. 3e, which was centered at 600 nm. The emission at this range was caused by two factors: the emission from the CDs and defects of ZnO. Meanwhile, the intensity of this emission was greatly decreased compared to that of bare ZnO prepared without using CMC. The abatement of ZnO@CDs emission may be caused by the CDs in composite, which can transfer the excited electrons right away from the conductive band and block the recombination of excited electrons and holes.

Figure 3f shows the PL spectra of ZnO/CDs at excitation wavelength of 350 nm. It can be observed that ZnO@CDs-160 and -180 gave the weakest emissions. Generally, high temperature may be favored by the decomposition of CMC, resulting in more CDs on ZnO. Thus, the uploaded dosage of CDs on ZnO@CDs-160 and 180 were higher, which can improve the carrier transfer rate and then enhance its photocatalytic property.

To further demonstrate the presence of CDs in ZnO@CDs, the fluorescence spectra (PL) of CDs, ZnO/CDs and ZnO at excitation wavelength between 260 to 450 nm were performed. Results are shown in Fig. 3g. Both emission intensities of CDs and ZnO/CDs showed excitation wavelength dependence, which is a characteristic of CDs. Meanwhile, the strongest emissions were centered at wavelengths of 450 to 500 nm, which originated from the CDs. ZnO showed almost the same intensity no matter how excitation wavelength changed. This gives evidence that CDs had been attached on ZnO in ZnO/CDs. Fluorescence pictures of CDs solution, ZnO suspension, and ZnO@CDs suspension were also taken under UV light irradiation (365 nm). It can be seen that both CDs solution and ZnO/CDs suspension had cyan color. The ZnO suspension had an orange color.

The mechanism of formation of CDs from MCC has been reported before (Wu *et al*. 2017; Mogharbel *et al*. 2023). MCC undergoes a breakage of glycosidic and hydrogen bonds and forms small organic acid molecules. After intermolecular dehydration, condensation and rearrangement among themselves, CDs are formed. CDs obtained formed the hydrothermal treatment of MCC, and some of the formed CDs have been attached on ZnO to form the ZnO/CDs composite.

Photocatalytic Activity

Photocatalytic experiments of hydrogen production under simulated sunlight irradiation were carried out with ZnO@CDs, where methanol was used as a sacrificial agent. Figure 4a shows the result of hydrogen production. All ZnO@CDs demonstrated good catalytic behavior for H_2 production. The hydrogen-producing capacity was 818 $\mu mol\cdot g^{-1}$ to ZnO@CDs-100. When increasing the preparation temperature, hydrogen-producing capacity of ZnO@CDs increased. It reached 1349 $\mu mol\cdot g^{-1}$ for ZnO@CDs-160. This is attributed to the fact that more CDs can upload on ZnO at high temperature, which improves the charge transfer efficiency, as illustrated in Fig. 4b. Compared to bare ZnO, the hydrogen production of ZnO@CDs-160 was 152% higher.

Meanwhile, samples of ZnO@CDs-160 and -180 displayed similar hydrogen production rates. To further understand the temperature influence on its photocatalytic property, the EIS (Electrochemical Impedance Spectroscopy) of ZnO@CDs was tested. In Fig. 4c, the radius of the Nyquist plot obtained from EIS test decreased with the increase of hydrothermal temperature. The ZnO@CDs-160 had the smallest radius of all the samples. Because the radius of the electrical impedance semicircle is related to the electron transfer rate, and the smaller the radius is, the higher the separation efficiency of the photogenerated carriers. This means ZnO@CDs-160 had the highest separation efficiency. It may be caused by the dosage of uploaded CDs on composite surface: high temperature can result in more CDs from the MCC. However, ZnO@CDs-180 had a larger semicircle compared to that of ZnO@CDs-160. This indicated that too many CDs may reduce the electrons transportation between the ZnO and CDs.

Compared with recent studies listed in Table 1, ZnO@CDs showed relatively good performance. Though GO/ZnO/CdS showed a higher H_2 production rate, ZnO@CDs had the advantage of low preparation cost and pollution-free sacrificial agent.

Table 1. Values of the H_2 Production Rate of Various Materials

Materials	Light Source	Sacrificial Agent	H_2 Production Rate ($\mu mol \cdot g^{-1} \cdot h^{-1}$)	References
ZnO@Au	300 W Xe lamp (ultraviolet cutoff)	Na_2SO_3 & Na_2S	120	Chen *et al.* 2020
ZnO@Ru	UV lamps	—	304	Vaiano and Iervolino
ZnO@MoS_2	300 W Xe lamp	Na_2SO_3 & Na_2S	235	Hunge *et al.* 2023
ZnO@ZnS	300 W Xe lamp	Na_2SO_3 & Na_2S	2400	Ren *et al.* 2022
ZnO@CdS	300 W Xe lamp (420 nm long pass	Na_2SO_3 & Na_2S	669.6	Guo *et al.* 2022
GO/ZnO/CdS	150 W lamp	Na_2SO_3 & Na_2S	6511	Chen *et al.* 2022
ZnO@CDs	300 W Xe lamp (AM1.5 filter)	Methanol	2480	This work

The fast decay of H_2 production was also observed. Take the ZnO@CDs-160 as an example, its hydrogen-producing capacity reached 1240 $\mu mol \cdot g^{-1}$ in 30 min; it was 1349 $\mu mol \cdot g^{-1}$ after 60 min. The values did not increase as expected. It appears that serious photo-corrosion happened on the surface of the composite. During irradiation, a large number of photogenerated holes were left in the filled band, which would enrich the outer surface of ZnO and attack the O atoms. These actions are expected to lower the photocatalytic performance (Huang *et al*. 2023; Khan *et al*. 2023).

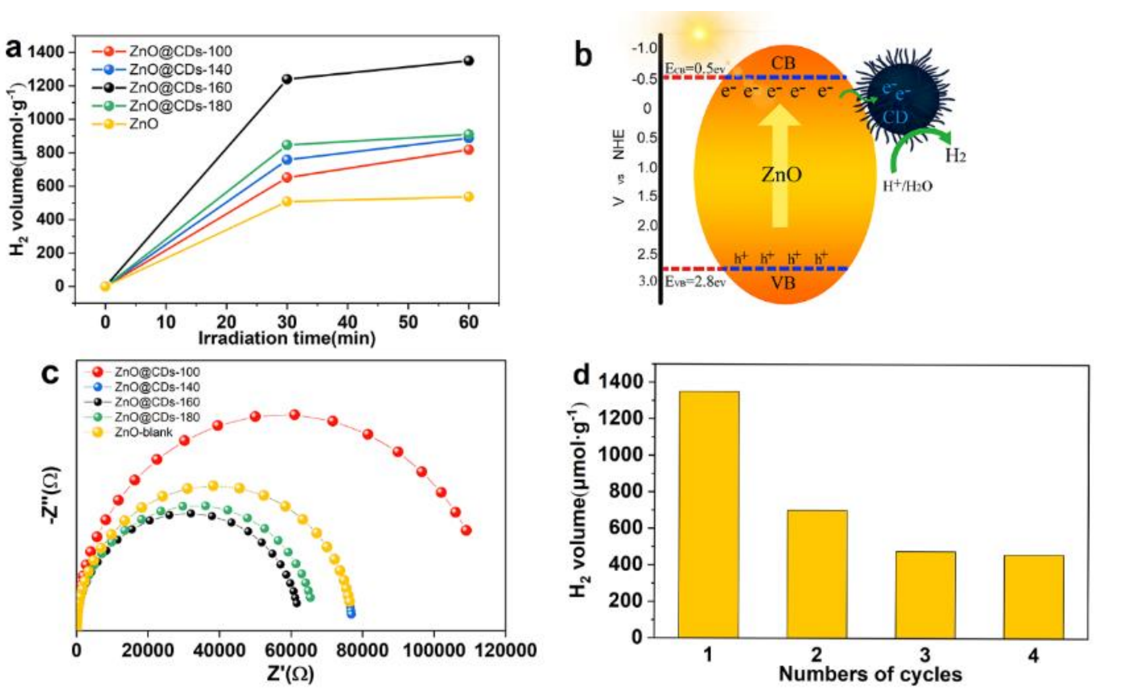

Fig. 4. (a) H_2 production of ZnO@CDs and ZnO under irradiation of simulated sunlight, (b) Illustration of electron transfer between ZnO and CDs, (c) Nyquist plot of ZnO@CDs and ZnO, (d) The cycling experiments of ZnO@CDs-160 for H_2 production

To test the stability of ZnO@CDs, cycling experiments of ZnO@CDs-160 were carried out, and the results are shown in Fig. 4d. It can be seen that the H_2 production decreased to 699.3 and 476.4 $\mu mol \cdot g^{-1} \cdot h^{-1}$, which was attributed to photo-corrosion. The H_2 production rate changed little in the 4th cycle, which means the ZnO@CDs became stable after running 3 cycles. Though photo-corrosion happened, the short-term catalysis of ZnO@CDs within the first 0.5 h was able to reach the total cumulative hydrogen production of a typical photocatalyst for more than several hours (Barman *et al*. 2017; Raza *et al*. 2023). Further work on solving photo-corrosion needs to be conducted.

CONCLUSIONS

1. A photocatalyst composite comprised of carbon dots loaded onto ZnO particles (ZnO@CDs) was prepared *via* hydrothermal synthesis and microcrystalline cellulose (MCC) was used as the raw material for preparation of CDs.
2. The CDs were able to improve the separate efficiency of photo-exited carriers and enhanced photodissociation of hydrogen from water.
3. The H_2 production was able to reach 1349 $\mu mol \cdot g^{-1}$ in 1 h under simulated sunlight irradiation, which was 152% higher than that of bare ZnO.

ACKNOWLEDGMENTS

The research received support from the National Innovation Training Programme for College Students at Northeast Forestry University (No. 2024) and Heilongjiang Province Philosophy and Social Science Research Planning Project (21YSE378).

REFERENCES CITED

Balanta, M. A. G., da, Silva Filho, W. J. F., Souza, M. C. G., de Assunçao, R. M. N., Champi, A., and Cuevas, R. F. (2023). "Deconvolution of photoluminescence spectra and electronic transition in carbon dots nanoparticles from microcrystalline cellulose," *Journal of Luminescence* 255, article 119607. DOI: 10.1016/j.jlumin.2022.119607

Barman, M. K., Mitra, P., Bera, R., Das, S., Pramanik, A., and Parta, A. (2017). "An efficient charge separation and photocurrent generation in the carbon dot–zinc oxide nanoparticle composite," *Nanoscale* 9(20), 6791-6799. DOI: 10.1039/c7nr90228j

Chauhan, I., Aggrawal, S., and Mohanty, P. (2015). "ZnO nanowire-immobilized paper matrices for visible light-induced antibacterial activity against *Escherichia coli*," *Environmental Science: Nano* 2(3), 273-279. DOI: 10.1039/c5en00006h

Chen, C., Huang, Y., and Huo, S. (2022). "Preparation and photocatalytic H_2 production property of graphene oxide/CdS/single crystal ZnO nanorod ternary hybrids," *Vacuum* 205, article 111467. DOI: 10.1016/j.vacuum.2022.111467

Chen, X., Lou, Y., Dayal, S., Qiu, X., Krolicki, R., Burda, C., Zhao, C., and Becker, J. (2005). "Doped semiconductor nanomaterials," *Journal of Nanoscience and Nanotechnology* 5(9), 1408-1420. DOI: 10.1166/jnn.2005.310

Chen, Y., Ma, L., and Ding, S. (2020). "Enhanced photocatalytic hydrogen generation by optimized plasmonic hot electron injection in structure-adjustable Au-ZnO hybrids," *Catalysts* 10(4), 376. DOI: 10.3390/catal10040376

Guo, X., Liu, X., Yan, J., and Liu, S. F. (2022). "Heteroepitaxial growth of core-shell ZnO/CdS heterostructure for efficient and stable photocatalytic hydrogen generation," *International Journal of Hydrogen Energy* 47(81), 34410-34420. DOI: 10.1016/j.ijhydene.2022.08.032

Guo, Y. R., Yu, F. D., Fang, G. Z., and Pan, Q. J. (2013). "Synthesis, structural characterization and photoluminescent properties of mesoporous ZnO by direct precipitation with lignin-phosphate quaternary ammonium salt," *Journal of Alloys and Compounds* 552, 70-75. DOI: 10.1016/j.jallcom.2012.10.035

Han, M., Zhu, S., Lu, S., Song, Y., Feng, T., Tao, S., Liu, j., and Yang, B. (2018). "Recent progress on the photocatalysis of carbon dots: Classification, mechanism and applications," *Nano Today* 19, 201-218. DOI: 10.1016/j.nantod.2018.02.008

Huang, F., Li, Z., Xu, Y., Yan, A. H., Zhang, T. Y., Wang, Q. D., Li, S. H., Lu, S. J., Zhao, W. X., and Gao, Y., *et al*. (2023). "Excellent anti-photocorrosion and hydrogen evolution activity of $ZnIn_2S_4$-based photocatalysts: In-situ design of photogenerated charge dynamics," *Chemical Engineering Journal* 473, article 145430. DOI: 10.1016/j.cej.2023.145430

Hunge, Y. M., Yadav, A. A., Kang, S. W., Lim, S. J., and Kim, H. (2023). "Visible light activated MoS_2/ZnO composites for photocatalytic degradation of ciprofloxacin antibiotic and hydrogen production," *Journal of Photochemistry and Photobiology A: Chemistry* 434, article 114250. DOI: 10.1016/j.jphotochem.2022.114250

Jamal, N., Radhakrishnan, A., Raghavan, R., and Bhaskaran, B. (2020). "Efficient photocatalytic degradation of organic dye from aqueous solutions over zinc oxide incorporated nanocellulose under visible light irradiation," *Main Group Metal Chemistry* 43(1), 84-91. DOI: 10.1515/mgmc-2020-0009

Khan, S., Poliukhova, V., Tamir, N., Park, J., Suzuki, N., Terashima, C., Katsumata, K. I., and Cho, S. H. (2023). "Dual function of rhodium photodeposition on ZnO/ZnS: Enhanced H_2 production and photocorrosion suppression in water," *International Journal of Hydrogen Energy* 48(26), 9713-9722. DOI: 10.1016/j.ijhydene.2022.12.045

Li, T., Zhao, D., Li, L., Meng, Y., Xie, YH., Feng, D., Wu, F., Xie, D. L., Liu, Y. X., and Mei, Y. (2023). "Unraveling fluorescent mechanism of biomass-sourced carbon dots based on three major components: Cellulose, lignin, and protein," *Bioresource Technology* 394, article 130268. DOI: 10.1016/j.biortech.2023.130268

Liu, K., Liang, H., Nasrallah, J., Chen, L., Huang, L., and Ni, Y. (2016). "Preparation of the CNC/Ag/beeswax composites for enhancing antibacterial and water resistance properties of paper," *Carbohydrate Polymers* 142, 183-188. DOI: 10.1016/j.carbpol.2016.01.044

Luo, J., Zhang, S., Sun, M., Yang, L., Luo, S., and Crittenden, J. C. (2019). "A critical review on energy conversion and environmental remediation of photocatalysts with remodeling crystal lattice, surface, and interface," *ACS Nano* 13(9), 9811-9840. DOI: 10.1021/acsnano.9b03649

Mogharbel, A. T., Abu-Melha, S., Hameed, A., Attar, R. M., Alrefaei, A. F., Almahri, A., and El-Metwaly, N. (2023). "Anticancer and microbicide action of carbon quantum dots derived from microcrystalline cellulose: Hydrothermal versus infrared assisted techniques," *Arabian Journal of Chemistry* 16(1), article 104419. DOI: 10.1016/j.arabjc.2022.104419

Nugroho, D., Wannakan, K., Nanan, S., and Benchawattananon, R. (2024). "The Synthesis of carbon dots//zincoxide (CDs/ZnO-H400) by using hydrothermal methods for degradation of ofloxacin antibiotics and reactive red azo dye (RR141)," *Scientific Reports* 14(1), article 2455. DOI: 10.1038/s41598-024-53083-3

Pan, J., Zhang, X., Zhao, C., Xie, S., Zheng, Y., Cui, C., and Li, C. (2018). "The flexible-transparent photosensitive films of cotton cellulose framework of carbon quantum dots/ZnO," *Materials Letters* 211, 289-292. DOI: 10.1016/j.matlet.2017.10.005

Raza, W., and Ahmad, K. (2022). "Graphitic carbon nitride-based photocatalysts for hydrogen production," in: *Sustainable Materials and Green Processing for Energy Conversion*, Elsevier, Amsterdam, Netherlands, pp. 213-236. DOI: 10.1016/B978-0-12-822838-8.00003-X

Raza, W., Ahmad, K., Khan, R. A., and Kim, H. (2023). "Ag decorated ZnO for enhanced photocatalytic H_2 generation and pollutant degradation," *International Journal of Hydrogen Energy* 48(75), 29071-29081. DOI: 10.1016/j.ijhydene.2023.03.406

Raza, W., Haque, M. M., and Muneer, M. (2014). "Synthesis of visible light driven ZnO: Characterization and photocatalytic performance," *Applied Surface Science* 322, 215-224. DOI: 10.1016/j.apsusc.2014.10.067

Ren, H., Ye, K., Chen, H., Wang, F., Hu, Y., Shi, Q., Yu, H., Lv, R., and Chen, M. (2022). "ZnO@ ZnS core–shell nanorods with homologous heterogeneous interface to enhance photocatalytic hydrogen production," *Colloids and Surfaces A: Physicochemical and Engineering Aspects* 652, article 129844. DOI: 10.1016/j.colsurfa.2022.129844

Tang, T., Zhao, J., Shen, Y., Yang, F., Yao, S., and An, C. H. (2024). "Carbon dots bridged Zn0. 5Cd0. 5S with interfacial amide bond facilitating electron transfer for efficient photocatalytic hydrogen peroxide production," *Applied Catalysis B: Environmental* 346, article 123721. DOI: 10.1016/j.apcatb.2024.123721

Trang, T. N. Q., Phan, T. B., Nam, N. D., and Thu, V. T. H. (2020). "*In situ* charge transfer at the Ag@ ZnO photoelectrochemical interface toward the high photocatalytic performance of H_2 evolution and RhB degradation," *ACS Applied Materials & Interfaces* 12(10), 12195-12206. DOI: 10.1021/acsami.9b15578

Vaiano, V., and Iervolino, G. (2019). "Photocatalytic removal of methyl orange azo dye with simultaneous hydrogen production using Ru-modified ZnO photocatalyst," *Catalysts* 9(11), article 964. DOI: 10.3390/catal9110964

Wang, Y. Y., Yu, H. Y., Yang, L., Abdalkarim, S. Y. H., and Chen, W. L. (2019). "Enhancing long-term biodegradability and UV-shielding performances of transparent polylactic acid nanocomposite films by adding cellulose nanocrystal-zinc oxide hybrids." *International Journal of Biological Macromolecules* 141, 893-905. DOI: 10.1016/j.ijbiomac.2019.09.062

Wang, Z. L. (2004). "Zinc oxide nanostructures: Growth, properties and applications," *Journal of Physics: Condensed Matter* 16(25), R829. DOI: 10.1088/0953-8984/16/25/r01

Wang, Z., Lee, Y. H., Kim, S. W., Seo, J. Y., Lee, S. Y., and Nyholm, L. (2021). "Why cellulose-based electrochemical energy storage devices," *Advanced Materials* 33(28), article 2000892. DOI: 10.1002/adma.202000892

Wu, P., Li, W., Wu, Q., Liu, Y., and Liu, S. (2017). "Hydrothermal synthesis of nitrogen-doped carbon quantum dots from microcrystalline cellulose for the detection of Fe^{3+} ions in an acidic environment," *RSC Advances* 7(70), 44144-44153. DOI: 10.1039/c7ra08400e

Wu, Z., Xu. C., Wu. Y., Yu, H., Tao, Y., Wan, H., and Gao, F. (2013). "ZnO nanorods/Ag nanoparticles heterostructures with tunable Ag contents: A facile solution-phase synthesis and applications in photocatalysis," *CrystEngComm* 15(30), 5994-6002. DOI: 10.1039/c3ce40753e

Ying, W., Liu, Q., Jin, X., Ding, G., Liu, M., Wang, P., and Chen, S. (2023). "Magnetic carbon quantum dots/iron oxide composite based on waste rice noodle and iron oxide scale: Preparation and photocatalytic capability," *Nanomaterials* 13(18), article 2506. DOI: 10.3390/nano13182506

Zhang, X., Xue, Y., Guan, Z., Zhou, C., Nie, Y., Men, S., Wang, Q., Shen, C., Zhang, D., and Jin, S., *et al*. (2021). "Structural insights into homotrimeric assembly of cellulose synthase CesA7 from *Gossypium hirsutum*," *Plant Biotechnology Journal* 19(8), 1579-1587. DOI: 10.1111/pbi.13571

Zhao, S. W., Zheng, M., Zou, X. H., Guo, Y. R., and Pan, Q. J. (2017). "Self-assembly of hierarchically structured cellulose@ ZnO composite in solid–liquid homogeneous phase: synthesis, DFT calculations, and enhanced antibacterial activities," *ACS Sustainable Chemistry & Engineering* 5(8), 6585-6596. DOI: 10.1021/acssuschemeng.7b00842

Zhao, Z., Reischauer, S., Pieber, B., and Delbianco, M. (2021). "Carbon dot/TiO_2 nanocomposites as photocatalysts for metallaphotocatalytic carbon–heteroatom cross-couplings," *Green Chemistry* 23(12), 4524-4530. DOI: 10.1039/d1gc01284c

Article submitted: April 8, 2024; Peer review completed: April 30, 2023; Revised version received: May 21, 2024; Accepted: June 19, 2024; Published: June 28, 2024.
DOI: 10.15376/biores.19.3.5511-5522